Low-cost reservoir tomographs of electrical resistivity

William Daily, Abelardo Ramirez, Robin Newmark, and Kenneth Masica, Lawrence Livermore National Laboratory, Livermore, California, U.S.

The geophysics we describe here will sound different from what you have heard before, because it is different. It uses electric fields instead of seismic waves. It is not designed for exploration. It is a distant cousin of cross borehole seismic tomography, although it is quite different in terms of its application and results. Probably the most curious aspect is that it doesn't chase the holy grail of geophysics—high resolution.

What good could possibly come from a low-resolution, electrical geophysical tool? The answer is found in the paradigm gradually finding favor by oil executives and reservoir engineers: while finding and exploiting large new fields is important for long-term growth, improving recovery efficiency for existing resources also makes sense because developing a new field is increasingly expensive. As a result, secondary recovery methods are receiving increasing attention.

This shift in view requires a parallel shift in geophysics. Now geophysics needs to deliver useful information about field production using low-cost, long-term monitoring techniques that have minimum impact on production operations. Electrical resistance tomography (ERT) is ideally suited to these new goals. ERT is a method for tomographically reconstructing the electrical resistivity distribution in the subsurface using an array of electrodes. Typically, current is driven between two of the electrodes and the resulting voltage distribution is measured on the remaining electrodes. Repeating this with other pairs of current electrodes in the array makes it possible to sample the subsurface electrical properties in a manner that allows calculation of the spatial distribution of those properties. The electrical properties depend strongly on pore fluid content. Consequently, ERT is especially good at giving information on the movements of oil, water, and gas—the principal fluids of interest in a petroleum reservoir.

An important aspect of this method is that the *oil well casings themselves are used as very long electrodes*. Normally, ERT surveys are conducted using a large number of electrodes, each one short compared to the distance separating them. We are advocating just the opposite—that the electrodes, each a steel casing, be very long compared to their separation—and, as we shall see, this strategy produces some interesting benefits. We call this synthesis of ERT and very long electrodes, long electrode electrical resistance tomography or LEERT (Daily and Ramirez, 1999). Figure 1 shows this simple concept.

What are those benefits of LEERT? First, and probably most important, is the fact that the electrodes are already scattered throughout the reservoir. No new "monitoring" wells are needed. Any well casing can be used as an electrode that reaches to the depth of the formation of interest. This means that the capital cost for doing LEERT is very small. Considering that the cost of a monitoring well can be as high as a million dollars, this advantage can make the difference between a method being practical or impractical and thereby the difference between used or not used.

A second benefit is that the well casing can be used irrespective of what else the well is used for or what it contains. It may be a production well, an injection well, or even a monitoring well and still be used as an LEERT electrode. The only real restrictions are that the casing must be steel (no insulators like fiberglass) and in good electrical contact with the formation. If it is a production well, then production tubing need not be removed for the casing for it to be used as an electrode. Production can continue uninterrupted. This, in fact, can be another significant cost benefit. Similarly, if it is an injection or monitoring well, its original function is unaffected.

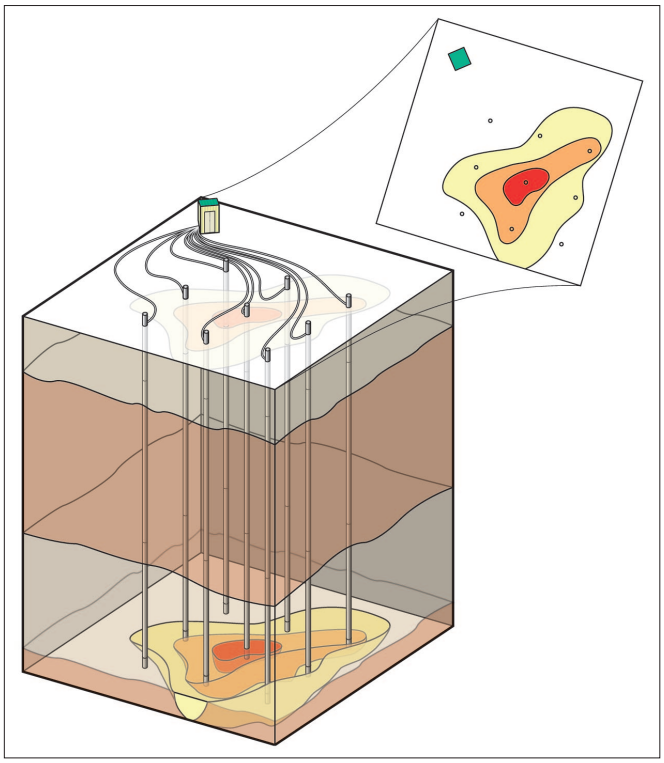

Figure 1. *LEERT concept. The long electrodes used for imaging reach into the formation to be imaged.*

A third benefit is that LEERT requires minimal field personnel to operate, thereby minimizing survey costs. Moving sondes in boreholes for logging or crosshole tomography, or moving sources and receivers on the surface for reflection seismology, are time consuming and expensive operations. The cost of a 3D surface seismic survey can reach $1 million (or more). Conventional borehole geophysics is less expensive but has an upfront cost and a downtime cost—as mentioned above. In contrast, the steel casings used by LEERT are all connected to a central multiplexer and are chosen automatically as a current source or for voltage measurement by an appropriate switching algorithm. It's all done automatically and with no moving parts.

For any monitoring method, the time interval between surveys is generally limited by the survey costs and the reluctance to remove wells from production. In contrast, we will show how LEERT can be used as a truly long-term monitoring tool able to yield nearly continuous imaging, not limited by mobilization costs, survey costs, downtime costs, or demobilization costs. We will show how LEERT can provide on-demand, real-time continuous imaging.

Commonly used borehole techniques tend to have a narrow field of view. For example, borehole logging is focused on a narrow strip around the well bore. Similarly, seismic crosshole tomography is insensitive to all but a narrow region directly between the well bores. In contrast, LEERT is a global tool, meaning that it is sensitive to the 3D volume in which the well casings are embedded and can provide a view of hundreds of acres of producing formation.

What is LEERT? Electrical geophysics was born when the Schlumberger brothers discovered that electric currents could be useful for probing the subsurface. Their methods were highly developed before the age of high-speed computing, but the technology direction took a sharp turn during the 1980s when high-speed digital computing became widespread. It suddenly became practical to solve electrostatic problems numerically that closely match reality. The power to quickly solve Laplace's equation and obtain the electrical response from a realistic numerical model made it practical to solve the inverse problem—that is, to calculate the numerical model which is appropriate to explain some real and specific data. The ability to solve the inverse problem removed much of the guesswork of traditional data interpretation which had previously been limited to matching measured data to a limited series of model-generated data. The new inversions made possible by high-speed computing were called tomography when applied to similar inverse solutions in other fields—the name also stuck here.

This inverse procedure produces a model (that is, a spatially varying distribution of resistivity) that gives an "acceptable" fit to the data and satisfies any other prescribed constraints. To find this model, we define an objective function that measures how well the numerical model reproduces the field measurements. Then the numerical procedure requires three elements: a forward model which computes transfer resistance given a 2D or 3D distribution of resistivity; an objective function which contains the model-fitting criteria used; and a search algorithm that uses the objective function to find the "optimum" resistivity model. Our objective function uses a smoothness operator that serves to stabilize the inversion by maximizing model smoothness. A more detailed description of the forward and inverse procedures used appears in the appendix.

Our interest is not a detailed description of reservoir static structure but rather a picture of reservoir changes resulting from movement of pore fluids. Therefore, the generalized inverse scheme is modified to calculate changes in reservoir properties. For this case, the data to be inverted (Z_i) are calculated from the measured impedances (Z_i (t_k), Z_i (t_k=0)) as follows:

$$Z_i = Z^h_j \, [Z_i \, (t_k) / Z_i \, (t_k=0)] \; (i = 1, \ldots, N)$$

where t_k is a specific time of interest, t_k=0 a time of baseline conditions, and Z^h the calculated transfer impedance for a homogeneous half space. When the electrical properties of the subsurface have not changed, then Z_i (t_k) = Z_i (t_k=0) and we are left to invert on Z_i for a homogeneous region which we arbitrarily set to unity.

The inverse problem is then solved for a layer of blocks coincident with the target formation horizons. If the process of interest is water flood, the inversion blocks form a layer at the injection depth. If the process is a steam or CO_2 flood, the inversion blocks are a layer at the zone of interest. Of course, if multiple zones are involved, then multiple layers of inversion blocks are included. All other parameter blocks are held constant at their initial value, arbitrarily set at unity (because they do not change).

Notice that this procedure results in information about the formation only within the layer (or layers) of blocks included in the inverse process. The inversion is therefore only two dimensional even though a three-dimensional forward model is used. This is a direct consequence of the fact that the electrodes are long compared to their separation. When the steel casings are vertical, the current flow is primarily horizontal so that there is very little information about vertical reservoir structure. All the vertical structure is built into the model from external information.

Any anthropogenic action designed to extract oil from the formation—ranging from primary production to stimulation of any sort—will usually change the electrical properties of the formation. These processes cause a change in pore fluid type and amount that is a primary factor affecting the formation's electrical properties.

Is it possible to image changes that might be caused by a steam flood, water flood, or just by production of oil? Is it possible to tell in which part of the field these processes are taking place? These are questions we want to answer.

LEERT from concept to field deployment. The development of LEERT has benefited from insight gained through numerical simulations and from measurements on laboratory scale models. Several questions had to be answered before the idea could be demonstrated in the field.

Numerical modeling. We first conducted numerical modeling studies to test the concept of using well casings as very long electrodes under ideal conditions. The purpose was to understand better the limitations of the approach, such as sensitivity. For example, is it possible to detect changes in a layer only 10 m thick that is buried 1000 m deep? Electrical resistivity changes in such a thin bed will alter the current flow near a well casing, but only over a very short length of such a long electrode. Sensitivity is proportional to the current density and only about 1% of the total current would enter such a thin layer so that its effect on measurable parameters will be small.

In addition, we needed to determine parameters that would constrain measurement system requirements. For example, it was necessary to estimate the transmitted current required to produce received voltages above the noise level. We expected that it would be necessary to supply relatively large currents (several amperes or more), because casings would have a very large surface area exposed to the formation. For example, a 3280-ft, 10-inch casing has a surface area in contact with the ground of more than 538 ft^2, making it an excellent grounding rod. Because the current is distributed over this entire area, the voltage gradients produced are small and sensitivity to changes in the formation is low.

Measurement system requirements. We had to determine the signal levels for what we expected would be a very difficult problem. For every ampere of current injected into the ground we expected the magnitude of the measured voltage (and especially their changes as the subsurface changed) to be substantially less than for applications using short electrodes. We had to know if these voltages were measurable at all with the noise environment expected in an oil field.

The calculations showed that (using the models shown in Figure 2 which we will describe below) for every ampere of current injected into the ground, the signals would range from 0.1 to a few millivolts. Although the exact values depend on many parameters such as the formation resistivity, the models we assumed yielded a range of voltages that should be fairly representative. A reasonable working current of 5 amperes (comfortable to work with moderately priced equipment) means signals of 0.5 to about 5 mv. Typical signal stacking time windows will yield a 100 microvolt noise level which leaves us with a signal to noise of 5 to 50.

Sensitivity to reservoir changes. A finite difference baseline model was generated to represent the relevant electrical properties (see Ramirez et al., 2003) of a nine-well pattern (20 acre with well spacing of 142 m) as shown in Figure 2 resulting in an image block 285 m on a side. The wells are 4880 ft deep with three 26-ft thick pay zones imbedded in a 100 ohm m

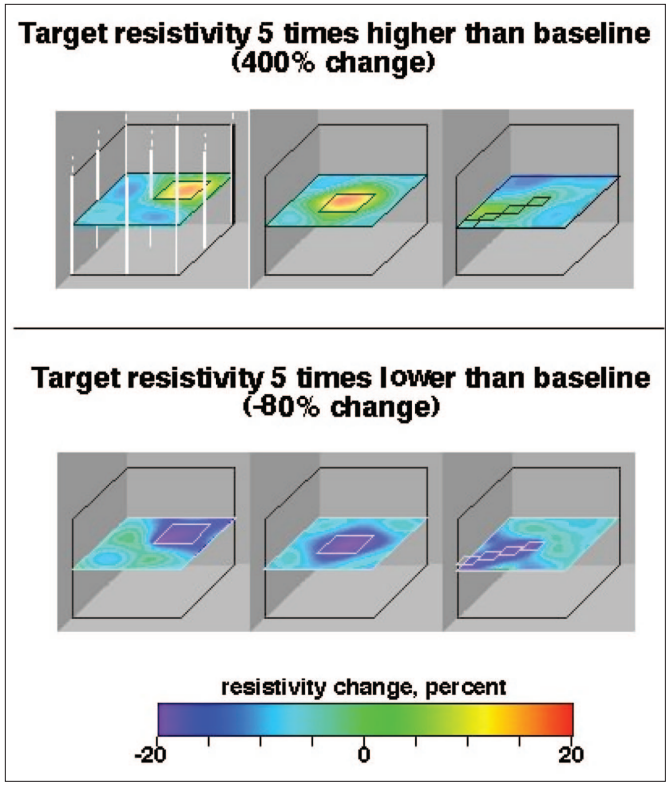

Figure 2. *ERT modeling for a resistivity anomaly in a nine-spot well pattern. In each case a resistive or conductive anomaly of the indicated shape is put into a single layer of voxels and the data that would be measured were numerically calculated using a 3D finite element mesh. These data were then inverted and compared to the inversion of the uniform baseline. Voxels above and below that plane of the anomaly do not change and are made transparent. The electrode wells, which continue to the surface, are shown on only the first image.*

background: two 10 ohm m layers and a 10 ohm m half-layer.

To yield images of specific cases in this perturbation model, we assume injection of supercritical CO_2 that produces anomalies of various shapes and sizes in the center layer. In a pilot CO_2 injection at Maljamar Field in Lea County, New Mexico, induction logs showed that the electrical resistivity of layers increased by about a factor of 5 during the flood (Albright, 1984). Based on these observations, we constructed two models of a rectangular anomaly and one model of a linear anomaly as shown in Figure 2 wherein the resistivity increased five times the initial value of 10 Ohm m to 50 Ohm m. The figure also shows the case, more appropriate for an anomaly produced by a steam flood, wherein the resistivity decreases by five times the initial value of 10 ohm m to 2 Ohm m. For two cases, the size of the rectangular anomaly remains constant but shifts to a different location. Also shown are results when the target shape is elongated to simulate a preferential flow path.

In each case a resistive or conductive anomaly of the indicated shape is put into a single layer of voxels and the data that would be measured was numerically calculated using a 3D finite element mesh. These data were then inverted and compared to the inversion of the uniform baseline. Voxels above and below that plane of the anomaly do not change and are made transparent. The electrode wells, which continue to the surface, are shown on only the first image. The top half of the figure shows the results calculated when the target resistivity is five times higher than background. The bottom half of the figure shows the results obtained when the target resistivity is five times lower than background. Conclusions for the resistive anomalies such as a CO_2 flood are similar to those for conductive anomalies such as brine injection or a steam flood in an oil-producing zone.

The results in Figure 2 provide answers to the following questions.

- Can the method be used to infer location of the flood? Figure 2 shows that the different positions of the rectangular anomaly in the two models can be distinguished. However, the details in shape such as the rectangular corners are not discernable. However, it is clearly possible to decide in which quadrant the anomalies reside.
- Can the method be used to reveal preferential flow pathways? Although smearing is clearly evident, it is possible to discern a "preferential path" type anomaly and even to conclude that the path is between the corner and center well. Even this smoothed inversion provides more information than is now typically available and could be very valuable to an engineer trying to optimize production or control some other process in a field.
- What causes all this smearing in the reconstructions? Nine electrodes provide only 18 linearly independent, four-electrode, measurements. To solve for the resistivity of 49 voxels, the reconstruction algorithm regularizes the problem by limiting the search to smooth models only. This is a fundamental limitation of the method that could be addressed only by adding more data to the problem or by changing the method of regularization. (There are several ways this might be accomplished but we will not pursue them here.) Another important limitation is that the long electrode tomographs have no vertical resolution. As a result, a single horizontal section through the medium is sufficient to analyze the tomograph because all horizontal sections are the same. The lack of vertical resolution eliminates the possibility of estimating the volumes of anomalies or of detecting vertical features such as caprock breaches by CO_2.

In summary the numerical modeling results showed that, under ideal conditions (e.g., noise-free data), it is possible to image simple anomalies. The results are low resolution, but it is possible to determine important features such as approximate size and location. It is even possible to differentiate some shapes. An important limitation is the lack of any vertical information—with only vertical long electrodes only lateral features are imaged. Second, unless the available data are very accurate, it will be impossible to duplicate the encouraging results of these simulations. Given noisy data, the inversion codes will return noisy results. We find that when transmitting 5 amperes we can expect subsurface processes to cause only millivolt order of magnitude changes. Success will require careful calibrations and aggressive signal stacking. The numerical modeling suggested that field implementation of the method would be challenging, but not impossible.

Sources of error. We know from the numerical modeling just discussed that changes in the measured voltages are expected to be small—for typical casing lengths only a few millivolts. Therefore, we must be concerned about sources of noise that could be a problem.

We have assumed to this point that each well casing is electrically isolated from all others except for the connection through the formation. However, unless the oil well is abandoned, it will be connected to pipes on the surface so that it can be used for producing or injecting some fluid. This connection could create an undesirable electrical path that must be broken. The simplest and surest method is to disconnect and physically separate the casing from the surface pipe. In many cases this is not a problem for the few hours needed for LEERT data collection. However, electrically isolating the

casing like this can be a nuisance; it does add operating cost and can cut into revenue.

An option without these drawbacks is to insert an electrically isolating section, made of fiberglass or polyethylene, between the well head and the steel pipe. This works as long as the fluid in the isolating pipe is a poor electrical conductor. The actual requirement is that the electrical conductance along this fluid path be small compared to that through the formation, $C_p << C_f$. If the isolating section of cross sectional area α and length λ, is full of a conducting fluid σ, then the requirement is

$$\sigma\,(\alpha/\lambda) << C_f$$

If the casings are 5000 ft long, C_f is about 0.2 S. For a 4-inch diameter isolating section filled with fresh water (σ= 0.2 S/m), then the section need be roughly 100 ft long to ensure that the electrical path through the pipe only accounts for 10^{-3} of the current. Likewise, if the section is filled with a water-oil mixture of σ = 0.02 S/m, the section need be only 10 ft long. These are reasonable lengths for an isolating section and if filled with a gas then the section may reduce to an insulating gasket inserted between two flanges. However, if the section is full of brine with σ = 2 S/m it would need to be 1000 ft long. The feasibility of installing these sections is determined by their cost and operational impact.

In the field examples we shall describe below, the casings were either not connected to any surface pipe or were connected by very long (over 1000 ft) fiberglass or polyethylene pipe. Therefore, the current flowing along the fluid column should be negligible.

There is another source of error that could be important—magnetotelluric currents induced in the formation by fluctuations in the earth's magnetic field. As these currents move through the earth they can produce voltage gradients of millivolts per km. One strategy for combating these signals is to take data during magnetically quiet times, typically just after dusk or just before dawn when these signals can be 10-30 times smaller than during midday. Another approach may be to record the telluric signals at a nearby site and subtract their effect from the LEERT data. To date, it has been sufficient to confine our data acquisition to geo-magnetically quiet times in order to minimize magnetotelluric errors.

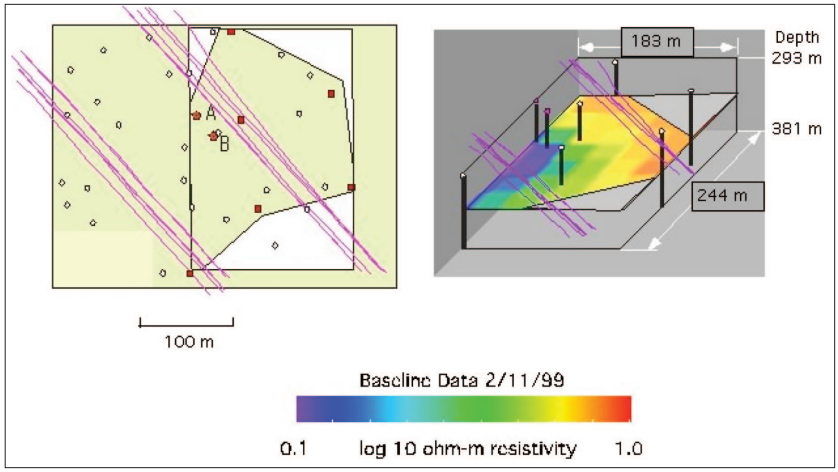

Figure 3. Borehole layout and the baseline image at Belridge Field. On the left is a plan view with the abandoned wells used as electrodes in red. White dots indicate the locations of production and stimulation wells that are in use, but not used for the LEERT survey. The parallel diagonal lines are the projection of horizontal production well onto the image plane. On the right, a perspective view of the baseline data of 11 February 1999, is shown with the relative location of the electrode wells.

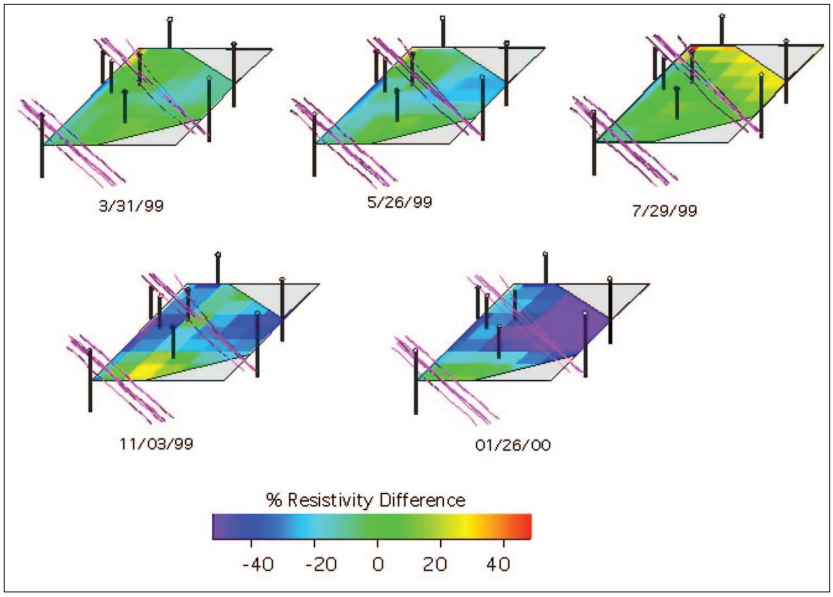

Figure 4. Perspective view of each ERT image is the pixel-by-pixel percent difference between the reconstruction for the date indicated and the baseline image (see Figure 3). The diagonal lines running through each image are the locations of horizontal production wells projected into each plane.

Operations at Belridge Field, Bakersfield, California—a steam flood. The first field deployment of LLERT was at a secondary recovery (steam flood) at Belridge Field near Lost Hills, California, U.S. The formation is shallow, only about 1250 ft, and our goal was simply to test components of the system under realistic field conditions. Issues to address included the small voltage changes expected (and our ability to detect them in the presence of typical oil field noise sources) and the placement and survival of several thousand feet of wire connecting the measuring system to wells in an active field.

The arrangement of wells we used as electrodes is shown in Figure 3. Six of these wells were abandoned so that their use as electrodes had no impact on regular operations in the field. The other two wells were actually installed especially for ERT but with a series of 30 independent electrodes in each array. To make each array work like a single long well casing, we simply connected all electrodes in each hole together so that at a little distance from each well, it behaved electrically like one continuous electrode.

Figure 3 also shows the baseline image of electrical resistivity taken on 11 February 1999. As we stated above, this 2D image doesn't represent the actual resistivity at any single depth but rather represents a composite of resistivity over the entire length of the electrodes. The baseline image reflects the reservoir response to ongoing stimulation operations. Steam flood had been ongoing in the southeastern portion of the field, with recent expansion to the northeast. The lower resistivity in the southwest portion of the field is consistent with these recent field operations.

The history of resistivity changes over the next 11 months is shown in Figure 4. The time lapse surveys present an interesting and believable picture for the response of the formation to the steam flood at depth. The type of pore fluid (oil, water, or gas), salinity, temperature, and formation saturation all play a role in the formation resistivity. It has been shown from model calculations and laboratory studies that in-situ resistivity can either increase or decrease as a result of steam flooding, depending on how these parameters change (Mansure and Meldau, 1989). However, a summary of field data by Mansure et al. (1993) shows that the formation resistivity almost always decreases during a steam flood. We can assume that a combination of increased temperature and additional pore condensate water combine to result in the usual case: a drop in formation resistivity during a steam flood.

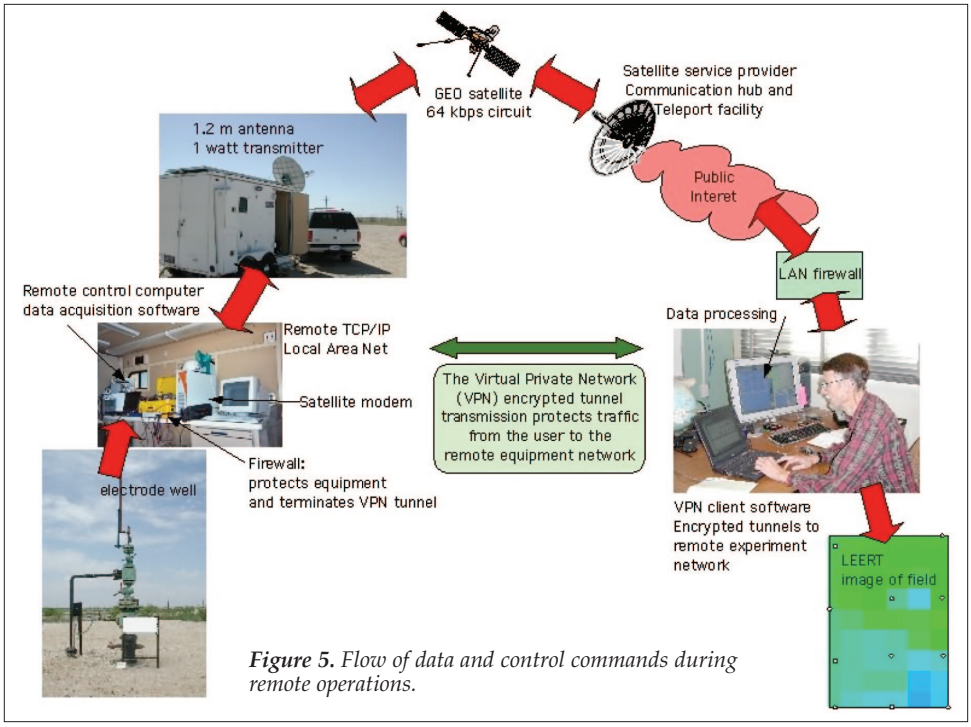

Figure 5. *Flow of data and control commands during remote operations.*

The very small but perceptible decrease in resistivity along the left edge and in the right corner of the March difference image are interpreted as early evidence of steam invasion into these areas since the February baseline. By May, these same locations have become even more conducting, implying a continuation of steam invasion. The trend is broken in the July image which shows relative increases in resistivity along the right edge. We discovered after processing these data that there were repeated boiler outages during the May-July period. An argument can be made that the July image could look more like the March image, but we are uncertain why the resistivity would actually rebound in July so as to be higher than March values. It may reflect the collapse of the steam front that had already been established when the baseline survey was obtained in February. The November image picks up the same trend as was indicated in March and May and so implies that the steam flood collapse was short-lived and that the invasion paths initiated earlier in the year were re-established in November. We point out, however, that the July-November sampling interval is about three months whereas the earlier intervals were only about two months. The last image, from January, continues the trend through the middle of this region—presumably as the flood progresses. Notice that the field in the lower left of the January 2000 image has not changed resistivity since March 1999. A reservoir engineer should be able to use this information to plan a strategy for encouraging a sweep of this region missed by the steam flood (confirmed by independent data). This is an example of how even a qualitative interpretation of LEERT images might be useful to a reservoir engineer.

Remote operation of ERT. One goal of this work is to reduce the cost of long-term monitoring (say 3-10 years) by using a single measurement system, operated remotely, to produce data for a large (hundreds of acres) area. We are suggesting that control of the system, through a land or satellite communications link, could set system parameters, initiate data collection, monitor system health, switch the system to waiting mode, and retrieve the data for processing. The system could be left in place for several years, saving considerable travel and manpower costs and allowing frequent sampling of the reservoir. A short demonstration of such a system was accomplished as part of our work at the next field demonstration site—Buckeye, New Mexico (to be discussed later). This was a relatively remote site and frequent data acquisition, requiring frequent site visits, was rather expensive.

The general-purpose communication system that we set up has the flexibility to support different kinds of remote experimentation or data gathering activity; this system is called GET-NET. The configuration is shown schematically in Figure 5. The remote local area network has a data acquisition and control laptop computer that front-ends the LEERT instrumentation. Through the firewall/virtual private network (VPN) device, the remote LAN is connected to the satellite network using an Internet protocol (IP)-enabled satellite modem that sits inside the equipment trailer. The modem establishes connections with the satellite system when the remote LAN needs to send or receive data. The modem connects to an outside satellite dish antenna attached to the top of the trailer.

After propagating over the geosynchronous satellite connection, the data traffic is routed over the public Internet at the satellite service provider's teleport facility. Once on the Internet, the traffic is then routed to the local network and individual computer system(s) at LLNL. The direction of IP traffic flow as described is then reversed when traffic is generated from LLNL and sent to equipment on the remote LAN. This hybrid Internet/satellite medium offers significant cost benefits over other options, and provides flexibility to access the remote equipment from an office, a lab, home, or wherever Internet access is available.

The cost for the ground station from the satellite vendor chosen was approximately $5000. This is a one-time cost for the customer, who then owns the equipment.

Because remote equipment is being interconnected over the public Internet and data is being sent over a large footprint geosynchronous satellite system, there was a need to incorporate network security features into GET-NET. Firewalls

were used to protect the remote LAN and provide filtering and separation from the satellite and Internet segments. VPN technology was used to encrypt and authenticate individual IP data packets flowing between LLNL and the remote LAN. Also, individual computers had usernames and passwords for user authentication.

In general, it can be challenging to get good performance out of a low-bandwidth VPN tunnel connection over a satellite using the IP protocol and a remote control application. Geosynchronous satellites, because of their position in high orbit, incur relatively significant propagation delays during the uplink and downlink transmission. However, such systems can be tuned and optimized in order to get adequate performance for interactive remote equipment control sessions. GET-NET is flexible and inexpensive and has allowed us to conduct remote experiments and collect data without the need for physical travel to the site. In addition, it can be located anywhere in the world because of the global reach of satellites.

Field operations at Vacuum Field—a CO_2 flood. Vacuum Field at Buckeye, New Mexico, a CO_2 flood in a producing oil reservoir, provided an opportunity to test the methodology at larger scale (wells farther apart) and deeper (longer electrodes and smaller signals). Because of its remote location, it also was a good place to test our ability for remotely controlled operation using GET-NET.

The well pattern is a 40-acre, 9 spot, and the producing formation, only 80-100 ft, is at a depth of approximately 5000 ft. Numerical modeling showed that the CO_2 induced data changes would range between 1.5 and 3.5% depending on the lateral extent of the flood. The borehole layout is shown in Figure 6. Baseline data were acquired in May 2002. Subsequent data were acquired in September and December 2002. Two comparison images are shown in Figure 6. As with the Bakersfield example discussed above, we use a simple qualitative interpretation of these results to demonstrate their utility.

The May-September interval (middle frame in Figure 6) shows little change in resistivity except for the lower right corner of the image which is becoming more conducting during this period. Most injected water is into wells 7 and 8. This steady water input could account for this conductivity increase if the water is displacing oil as it moves toward well 11. In addition, if this water is displacing oil, then we expect to see oil at 11 and indeed, in this part of the field, oil production is highest. The relative stability over the rest of the region is consistent with the low injected volumes and low produced volumes in the other wells in this area.

The next time interval, May-December (right frame in Figure 6), shows changes that continue the trend around wells 7, 8, 10, and 11 with that feature stronger and larger in size. However, there is now a new larger conductive anomaly centered on well 4 and a small resistive anomaly near well 8. The resistive anomaly near well 8 may be a result of a large gas bubble. We postulate that such could form as a combination of two factors. First, water injection was terminated in well 8 and simultaneously a large increase in gas (methane) was seen in several of the production wells but was especially large for the well in the pattern directly adjacent to well 8. The hypothesis is that as the water pressure dropped, electrically conductive water was replaced by electrically resistive gas, creating a gas bubble near well 8.

The conducting anomaly surrounding well 4 is more difficult to explain. It may be related to the large gas production spike that occurs between September and December. If this spike is a result of a wide-spread (observed in all production wells in the neighborhood) pressure disequilibrium in the formation, then fluid movement in response to the gas production could have likewise been widespread.

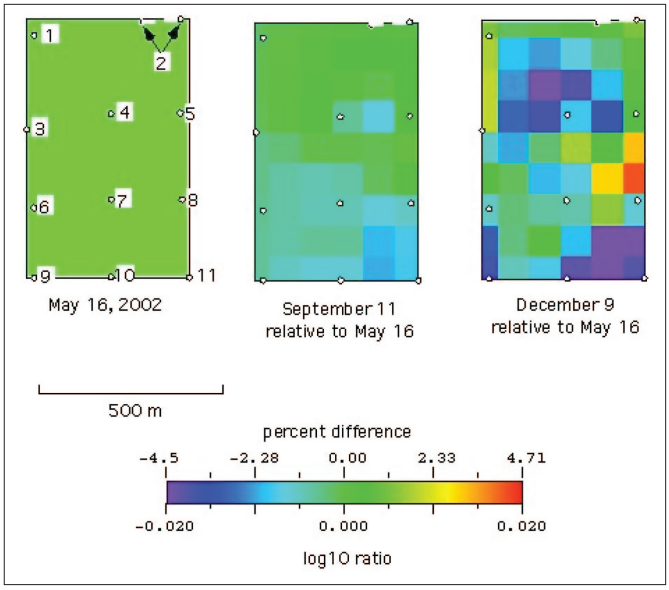

Figure 6. Results from monitoring the CO_2 flood for seven months. On the left is the well layout showing the boundary of the image reconstruction area. The center and right show changes in resistivity between the May 16 baseline and September 11 and December 9, respectively. Well 2 was not vertical, and its actual trace was modeled in the 3D finite difference mesh.

None of these scenarios invokes the movement of CO_2. This is most likely because up to the end of the usable data very little CO_2 had been added to this portion of the field. Most injected CO_2 went to well 1 but really small amounts went intermittently to wells 2 and 6.

Summary and conclusions. Over the past few years we have developed a new geophysical tool called long electrode electrical resistance tomography, or LEERT. The tool combines familiar methods of electrical resistivity measurements and tomographic inversion with the new but simple idea of using very long steel well casings as electrodes. The new method can be used to map pore fluid changes caused by primary and secondary recovery processes in very deep reservoirs and over very large areas.

Using numerical modeling we have explored the sensitivities of the method and its practical limitations. Because the signals are very small, it is necessary to make very accurate measurements. This means that to monitor processes that occur over periods of years a very stable measurement system is required. In addition, errors such as telluric noise must be kept to a minimum. Methods have been developed to deal with these and other difficulties.

At the onset of the project, we appreciated the fact that it was one thing to make LEERT work "in the computer" but it would be quite another matter to make it work under realistic conditions. As a result an important part of this work was to test the lessons learned from computer modeling at two field sites, and both have taught us very useful lessons. The first site was a relatively shallow steam flood and the second was a deeper CO_2 flood. At both sites it was possible to map the spatial and temporal distribution of electrical resistivity resulting from deep fluid movement.

As a bonus, during the year-long deployment at the CO_2 flood site, we developed the ability, using a commercial satellite Internet link, to control the LEERT data acquisition system remotely. With this link it was possible to take data on

command and retrieve the data for processing, from the author's office in California—all without sending a crew to the field site. This capability has obvious beneficial impact on the cost of and future use of LEERT.

This new tool has the capability of imaging moderately deep processes that change the electrical properties of a reservoir provided the process being monitored produces sufficient electrical contrasts in the formation. There are trade offs between depth, formation contrasts, and formation thickness. The method becomes easier for shallow, thick formations that experience large changes in electrical conductivity. The feasibility to map reservoir changes at a specific site can be determined in advance using readily available computational tools.

Advantages of LEERT include the low capital cost and low impact on field operations. Sampling the formation can almost always be accomplished using existing wells as long as they are cased deep enough to penetrate the formation of interest. If production or injection wells are used, pulling tubing is not required although it is sometimes necessary to shut in a well for 2-3 hours for data acquisition. Usually, no additional or specialized wells, such as monitoring wells, are required. LEERT can be very compatible with normal field operations. In addition, both the capital and operational costs of LEERT measurement equipment are relatively small. Commercial data acquisition systems are currently available for around $40 000. Remote operation over a commercial satellite link translates into low operational costs—very few times a crew is necessary on-site. Data goes directly to a central processing computer where it is processed without human intervention until interpretation is needed at the final result. The method is especially good for long term monitoring with near-real-time data processing of many closely spaced sampling intervals.

The method has limitations. Most noticeable is the low spatial resolution in the imaging. Resolution will vary depending on the number and spatial distribution of wells, and the signal-to-noise ratio of the data, but a rule of thumb is that spatial resolution will be approximately one third to one half the typical well spacing. If steam is injected into a well, it will be possible to tell which direction the steam front is moving and about how fast by examining several images, but details about flow channel structure will be unavailable. Also, the method will only show horizontal features using only vertical wells and is unable to yield any information about vertical movement of fluid. There is also a perception disadvantage resulting from the fact that production engineers know and trust long proven seismic methods and service contractors. Seismic methods have been highly developed and often yield high-resolution results—LEERT is not a seismic method.

We do not expect that LEERT will replace currently valuable methods, but it can supplement them, especially in situations where low-cost, long-term monitoring is of interest. In addition, LEERT could be used to constrain the solution space searched by the reservoir simulation algorithms that are routinely used by engineers to better understand and predict reservoir behavior.

Suggested reading. "Use of well logs to characterize fluid flow in the Maljamar CO_2 pilot" by Albright (SPE 1984 Annual Technical Conference and Exhibition). "Occam's inversion of 3D ERT data" by LaBrecque et al. (*Proceedings of the International Symposium on Three-Dimensional Electromagnetics*, 1995). "Steam-Zone electrical characteristics for geodiagnostic evaluation of steam flood performance" by Mansure and Meldau (SPE 18797, XPE California Regional Meeting, 1989). "Field examples of electrical resisivity changes during steam flooding" by Mansure et al. (SPE Formation Evaluation, 1993). "Monitoring sequestered carbon dioxide floods using electrical resistance tomography (ERT): Sensitivity studies, Lawrence Livermore National Laboratory" by Ramirez et al. (*Journal of Environmental and Engineering Geophysics*, 2003). *Solutions of Ill-Posed Problems* by Tikhonov and Arsenin (Winston and Sons, 1977).

Acknowledgments: This work was made possible by our partners: ChevronTexaco, TOMOseis, and SteamTech Environmental Services. Support in the field work was provided by Wayne Minchew and Steve Jackson (ChevronTexaco), Hank Sowers (SteamTech), and many others. LLNL colleagues Dwayne Smith, David Ruddle, and Brian Mitchell assisted in field operations. This work was funded by the U.S. DOE Natural Gas and Oil Technology Partnership, U.S. Office of Basic Energy Sciences, and the U.S. DOE National Energy Technology Laboratory. This work was performed under the auspices of the U.S. Department of Energy by University of California Lawrence Livermore National Laboratory under contract W-7405-Eng-48.

Corresponding author: daily1@llnl.gov

Appendix: Modeling and inverse methods. The forward problem is solved using a 3D, finite-difference technique described by LaBrecque et al. We use the finite difference method with rectangular, hexahedral elements to convert the potential differential equation into a system of linear equations. Within each element, electrical conductivity is constant. The algebraic equations produced by the finite difference method are of the form:

$$\underline{G}V=I \tag{1}$$

where $\underline{G}$ is an M by M matrix, V is a vector of the estimated potential at nodes, I is a vector of the current injected at selected nodes, and M is the number of mesh nodes.

Highly conductive structures such as metallic casings are modeled by lowering the conductances in the matrix along columns (or rows) of nodes in the finite difference mesh. The value of the conductances between such nodes is calculated using the diameter and electrical resistivity of the casing material and the modified conductance values remain fixed during inversion.

The three-dimensional inverse algorithm is described by LaBrecque et al. (1995). Three-dimensional inversion is, by nature, strongly underdetermined. Inverse solutions that consider only the fitting of the forward model to field data are nonunique. Therefore, the algorithm uses a regularized solution (Tikhonov and Arsinen, 1977) that jointly minimizes the misfit of the forward model to the field data and stabilizes the inverted value of the parameters. To find the optimal value of the parameter vector **P**, the algorithm finds the maximum value of α, the stabilization parameter, for which minimizing:

$$\Upsilon(\mathbf{P}) = \chi^2(\mathbf{P}) + \alpha \mathbf{P}^T \underline{\mathbf{R}} \mathbf{P} \tag{2}$$

results in:

$$\chi^2(\mathbf{P}) = \chi^2_{prior}. \tag{3}$$

The parameters, **P**, are the natural logarithms of the conductivity of the mesh elements. In equation 2, we use $\underline{\mathbf{R}}$, the solution roughness, as the stabilizing functional. Also in equation (2), χ^2_{prior} is equal to the number of data points and χ^2 is given by:

$$\chi^2 = (\mathbf{D} - \mathbf{F(P)})^T \underline{\mathbf{W}} (\mathbf{D} - \mathbf{F(P)}) \tag{4}$$

where **D** is the vector of known data values, **F(P)** is the for-

ward solution and $\underline{\mathbf{W}}$ is a data weight matrix. The diagonal elements of $\underline{\mathbf{W}}$ are the reciprocals of the data variances and the off-diagonal elements are zero. This assumes noncorrelated data errors.

We note that for a given α, usually one P vector will yield the desired. This means that the approach can produce a unique solution given the roughness parameter used. The roughness operator α controls the relative weighting of roughness (the inverse of smoothness) and data fitting in the objective function. It helps stabilize and remove ambiguity in the resistivity inversion by minimizing the model roughness (maximizing model smoothness). This operator in a very real sense trades off resolution and sensitivity for inversion robustness. This means that the inversion process can be tuned to be very robust or to fit the data very accurately, but both goals cannot be accomplished equally well at the same time. In actual practice, the α estimator used aims to achieve a balance between these two goals. In typical problems, it produces resistivity models that exhibit minimum roughness while fitting the data to a prescribed prior tolerance. TLE